Germanium concentration associated to sphalerite recrystallization: an example from the Pyrenean Axial Zone

Alexandre Cugerone, Bénédicte Cenki-Tok, Emilien Oliot, Manuel Munoz, Alain Chauvet, Fabrice Barou, Kalin Kouzmanov, Stefano Salvi, Vincent Motto-Ros, Elisabeth Le Goff

Germanium concentration associated to sphalerite recrystallization: an example from the Pyrenean Axial Zone

Alexandre Cugerone, Bénédicte Cenki-Tok, Emilien Oliot, Manuel Munoz, Alain Chauvet, Fabrice Barou
Géosciences Montpellier

Kalin Kouzmanov
University of Geneva

Stefano Salvi
Géosciences Environnement Toulouse

Vincent Motto-Ros
Institut Lumière et Matière

Elisabeth Le Goff
Bureau de Recherches Géologiques et Minières (BRGM)

Abstract. Germanium (Ge) is often found as trace element in undeformed sphalerite (ZnS). However, the presence of Ge-minerals (oxides, chloritoids and/or sulphides with up to 70 wt% Ge) is remarkable in Pb-Zn deposits from the Variscan Pyrenean Axial Zone. Their abundance is controlled by the chemical and/or the mechanical processes that affect rare element concentration from sulphides which have undergone deformation and metamorphism. In this study, we document the microstructures and chemical heterogeneities in sphalerite, based on EBSD (electron backscatter diffraction) coupled to LA-ICPMS *in situ* analyses. Deformation induces the dynamic recrystallization of sphalerite. Recrystallized domains have low Ge contents (1–50 ppm Ge) whereas porphyroclastic sphalerite grains commonly show higher Ge concentrations (up to 650 ppm Ge). Ge-minerals (up to 70 wt% Ge) are exclusively hosted by the Ge-poor recrystallized domains. We propose that Ge was removed from the sphalerite crystal lattice during sulphide recrystallization, and was subsequently concentrated in Ge-minerals, leaving behind a Ge-depleted fine-grained recrystallized sphalerite matrix. Numerous sulphide ore types enriched in rare elements like Pyrenean deposits may present recrystallization features and we suggest evaluating the potential of such deposits by integrating chemical and structural informations at the micrometer scale using state-of-the-art analytical techniques in exploration methods.

1 Introduction

Critical metals like Germanium (Ge), Gallium (Ga) or Indium (In) are often accommodated by the sphalerite lattice (Cook et al. 2009). These elements are presently exploited as by product in base metal deposits in low concentrations (up to several 1000s ppm ; Höll et al. 2007) as commonly observed in non-deformed sulphides (Cugerone et al. 2018a). However, the highest concentrations of zinc sulphide are hosted in deformed/metamorphosed environments (Wilkinson 2013), but the presence of critical metals in these deposit-type has been poorly explored.

The impact of recrystallization on sulphide composition has been mostly studied in pyrite or arsenopyrite (Cook et al. 2013; Dubosq et al. 2018) and only few studies are available for sphalerite (e.g. Lockington et al. 2014; George et al. 2016). Lockington et al. (2014) compare diverse sphalerites that naturally endured different metamorphic imprints. A loss of trace elements like Pb, Bi, Ag is commonly observed associated to a re-incorporation of Fe, Cd, Mn, In. Homogenization of Cu in the sphalerite lattice is observed but data concerning Ge incorporation in sphalerite are lacking.

The studied sphalerites are located in the Pyrenean Axial Zone (PAZ) Pb-Zn district deposits. These Pb-Zn mineralizations were sampled from deposits mined in the past and represent an interesting natural material for studying the impact of orogenic deformation on sphalerite texture and chemistry. The occurrence of Ge-minerals such as brunogeierite [$GeFe_2O_4$], briartite [$GeCu_2(Fe,Zn)S_4$] or carboirite [$GeFeAl_2O_5(OH)_2$] hosted in sphalerite has been reported in the PAZ (Johan et al. 1983; Cugerone et al. 2018a)

Combining textural (EBSD) and chemical (EPMA and LA-ICP-MS) analyses, our study aims at investigating the role of deformation/recrystallization on the behavior of trace elements in sphalerite, and, in particular the formation process of Ge-minerals.

2 Methods

Electron-BackScattered Diffraction (EBSD) maps were performed with a Camscan Crystal Probe X500FE SEM-EBSD at Geosciences Montpellier (CNRS-University of Montpellier, France). Operating conditions were 20 kV for the accelerating voltage and ~5 nA for the probe current with a working distance of 25 mm under 2 Pa low vacuum. Samples were positioned horizontally and at the standard 70° angle of the EBSD detector. EDS maps were acquired simultaneously with electron backscatter pattern data. The measurement step was systematically

below 5 µm. Oxford Instruments Aztec and Channel 5 softwares were used to generate EDS and EBSD maps.

Electron microprobe analyses (EMPA) were carried out using a Cameca SX100 (at the Service Inter-Regional Microsonde-Sud; Montpellier). Major, minor and trace elements were measured with a beam current of 100 nA and accelerating voltage of 20 kV. 14 elements were analyzed: standards, spectral lines, and spectrometers were as follows: Zn (Zn, L_α, TAP); S (FeS_2, K_α, PET); Fe (Fe_2O_3, K_α, LLif); Cd (CdS, L_α, LPET); Ge (Ge, K_α, LLif); Sb (GaSb, L_α, LPET); Cu (CuS, K_α, LLif); Ga (GaSb, K_α, LLif); Ag (Ag, L_α, LPET); Mn (Mn, K_α, LPET); Sn (Sn, L_α, PET); Pb (Pb, M_α, PET); As (GaAs, Lα, TAP); Si ($CaSiO_3$, K_α, TAP). Peak counting times ranged from 30 to 240 s (240 s for Ge). Germanium is analyzed on 2 LLif monochromators. The limit of detection for Ge and Cu, calculated by internal Cameca procedures, is reduced to 84 ppm and 110 ppm respectively. Ga, As, Ag, Pb, Sn, Sb, and Mn were below detection limit.

Laser ablation inductively coupled plasma-mass spectrometry (LA-ICP-MS) was used to determine trace elements concentrations in sphalerite. Analyses were carried out using an Excimer CompEx 102 coupled with a ThermoFinnigan Element XR available at the OSU-OREME AETE platform at the Montpellier University.

Laser ablation was performed at constant 5 Hz pulse rate with 140 mJ laser energy. Each measurement comprises 180 s of background measurement and 60 s of sample ablation (signal measurement), followed by a 60 s retention time to ensure a proper cell washout. Data were processed using the Glitter 4.0 software package. The following isotopes were measured: ^{29}Si, ^{34}S, ^{55}Mn, ^{57}Fe, ^{59}Co, ^{61}Ni, ^{63}Cu, ^{65}Cu, ^{64}Zn, ^{69}Ga, ^{71}Ga, ^{74}Ge, ^{75}As, ^{77}Se, ^{95}Mo, ^{105}Pd, ^{107}Ag, ^{109}Ag, ^{110}Cd, ^{111}Cd, ^{115}In, ^{118}Sn, ^{119}Sn, ^{120}Sn, ^{121}Sb, ^{123}Sb and ^{208}Pb. Zn contents in sphalerite measured with EPMA were used as internal standard of the LA-ICP-MS analyses. MASS-1 reference was used as external standard (Dr. Stephen Wilson, personal communication) with a corrected 57 ± 1.75 ppm value for Ge. NIST SRM 610 was used as secondary external standard to identify possible instrumental drift. Ni, As, Mo, Se, Pd and Si concentrations were systematically below detection limits. Only Ge and Cu contents measured in sphalerite will be discussed in this paper.

3 Pb-Zn deposits in the Pyrenean Axial Zone

Pyrenean Pb-Zn deposits are hosted in the deformed Variscan (~325-290 Ma) Pyrenean Axial Zone exhumed during the collision between the Iberia and Eurasian plates since the Lower Cretaceous. Foliation trajectories exhibit a monotonous N080-N110°E trend with variable dip angles. Two main Variscan deformation events are recorded in the host-rock. A poorly expressed S_1 cleavage is often parallel to original stratification S_0 and is associated to regional M_1 Medium-Pressure Low-Temperature (MP-LT) metamorphic conditions. A well-expressed S_2 cleavage is sub-vertical and superimposed to the previous structures. S_2 axial planar cleavage is associated to M_2 contact (HT-LP) metamorphic conditions, marked in the studied area with the appearance of cordierite.

Three Pb-Zn types of mineralization types are present in the PAZ and fully described in Cugerone et al. (2018b).

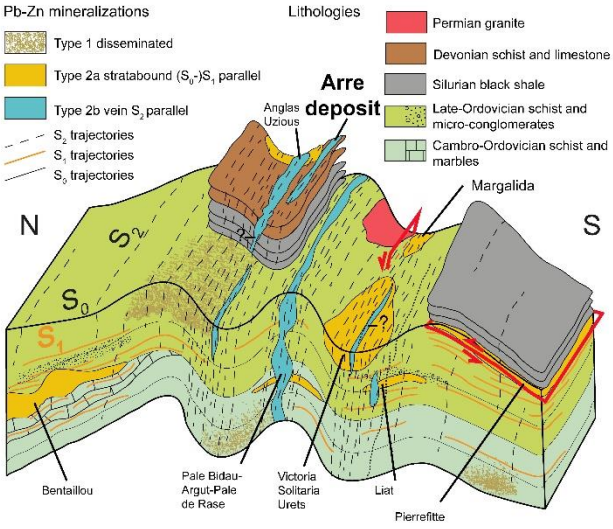

Figure 1: Schematic 3D sketch presenting the three main types of mineralization which are typically observed in the studied area and related to each studied deposit. Type 2b vein mineralizations appear in intensely S_2 deformed domains. Location of Arre deposit is noted (modified from Cugerone et al., 2018b)

In Figure 1, a schematic 3D sketch is shown and illustrates the major types of mineralization types. Type 1 corresponds to a minor disseminated mineralization, probably syngenetic and from an exhalative source. Type 2a is a stratabound mineralization, epigenetic and synchronous to the Variscan D_1 regional deformation event and (III) while Type 2b is a vein mineralization, epigenetic and supposed synchronous to the late Variscan D_2 regional deformation event.

Herein, we will only focus on the Type 2b Ge-rich mineralization and more precisely on Arre deposit (Cugerone et al. 2018b). Type 2b is an epigenetic sub-vertical vein-type mineralization (Fig. 2A) which has endured at least one deformation event, probably Variscan in age (D_2 in Cugerone et al. 2018b). These veins are composed of sphalerite and galena, with a small amount of pyrite, chalcopyrite, arsenopyrite and gangue of quartz-carbonate (Fig. 2B). Numerous Type 2b deposits are present in the Axial Zone (Cugerone et al. 2018b) and in this paper, we will focus on the Arre deposit. This Pb-Zn(-Ge) mineralization is hosted in Devonian calc-schist and marble rocks. Veins are oriented N070 E with sub-vertical dip (Fig. 2A).

4 Microstructural study

EBSD has been performed on Type 2b mineralizations (Fig. 3A and 3B) to obtain textural and microstructural information. Sphalerite occurs with diverse grain size (from 10 µm to > 1 mm). Coarse grains are parent grains and are internally deformed. Smaller grains (< 100 µm) mantled parent grains and also locally occur in twin boundaries. Three different textures are distinguished in

sphalerite: dark domains and light domains that are observed in coarse parent grains and recrystallized domains that are composed of newly formed smaller grains.

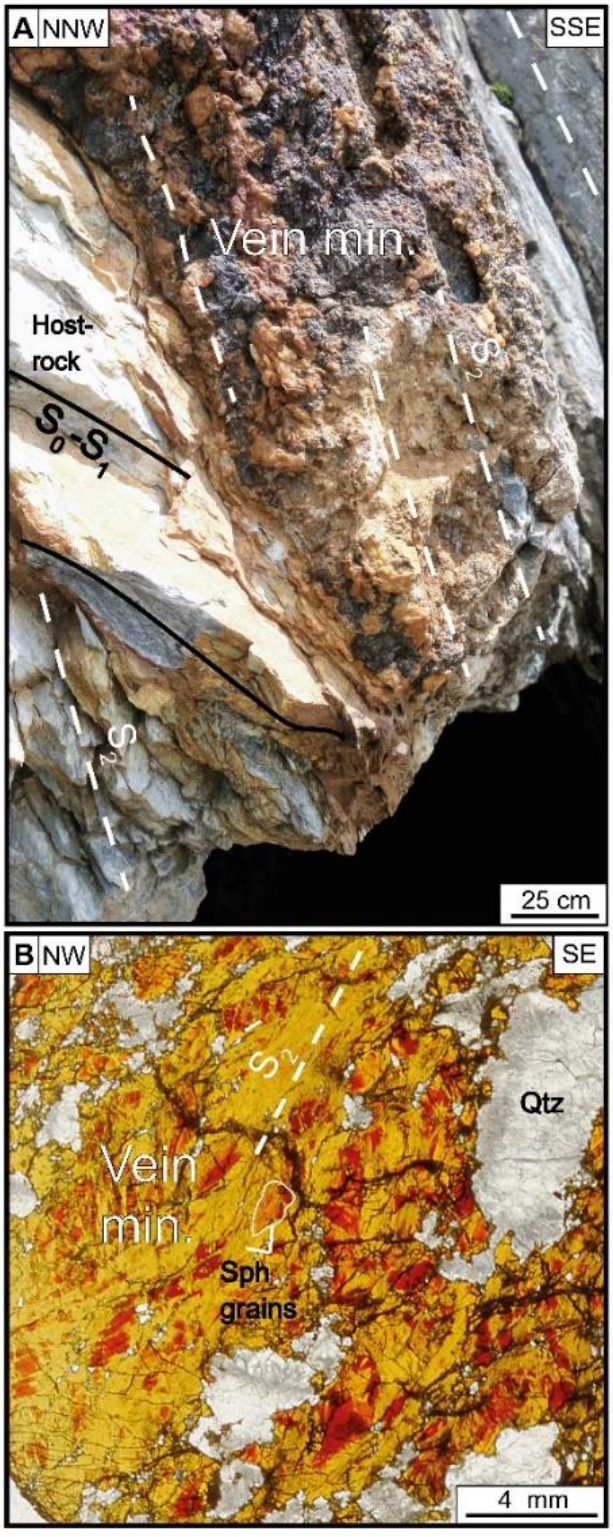

Figure 2: A: Pb-Zn Type 2b Vein in Arre deposit. B: Typical Pb-Zn Type 2b ore mineralization with color zonation in sphalerite and presence of superimposed S_2 cleavage (modified from Cugerone et al., 2018b; S_0-S_1: S_0-S_1 foliation; S_2: S_2 foliation; Qtz: quartz; Sph: sphalerite.

In the same area, an EDS chemical map is performed simultaneously to the EBSD acquisition, and so that the locations of Ge-minerals are reported (Figure 3A, yellow

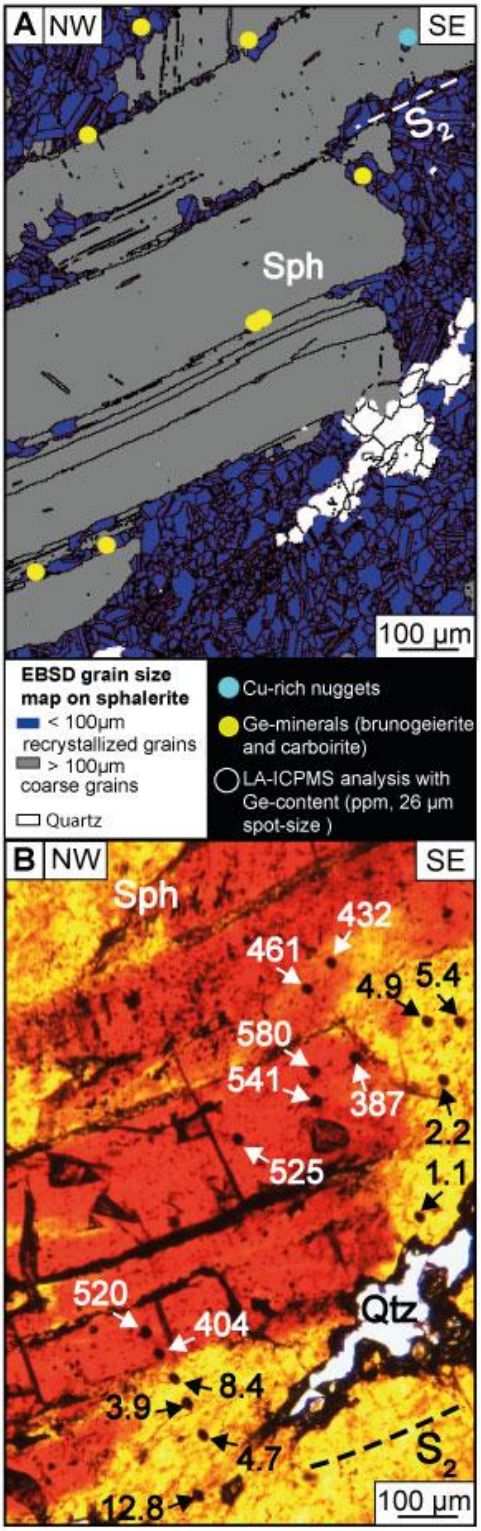

Figure 3. A: EBSD grain size map in sphalerite (Arre sample) with location of Ge and Cu rich phases. These minerals are preferentially located in recrystallized sphalerite domains. B: Corresponding area in transmitted light with LA-ICP-MS spot analyses associated to Ge-contents (in ppm). Note that the contrasts in color observed in Sph correspond to variations in Ge content. (S_2: S_2 foliation; Qtz: quartz; Sph: sphalerite).

dots). Ge-minerals mainly consist of brunogeierite ($GeFe_2O_4$) and carboirite ($GeFeAl_2O_5(OH)_2$); they are preferentially hosted in the small recrystallized sphalerite grain or located close to twin boundaries.

4 Ge and Cu in sphalerite

The location of LA-ICP-MS spot analyses was based on the EBSD grain size map so that chemical and textural information can be link each other. LA-ICP-MS spots are indicated in Figure 3B associated to their Ge-contents in zoned sphalerite as observed in transmitted light. Germanium distribution is highly zoned. In dark and light domains, the median content reaches 433 ± 21 ppm and 46 ± 2 ppm, respectively. In recrystallized domains, Ge content is typically low, with median Ge content is much lower with a median concentration of 4 ± 2 ppm. Heterogeneous Ge in sphalerite is positively correlated to Cu, especially in the dark and light domains with Cu median contents of 1012 ± 75 ppm and 102 ± 7 ppm respectively. Cu content is lower in recrystallized grains with a median value of 29 ±9 ppm.

A mass balance calculation performed between the different Ge-bearing phases observed reveals an "equivalent" Ge concentration in primary non-deformed sphalerite of 700 ppm in average (Cugerone et al., in prep).

5 Discussion and conclusions

The studied sphalerites from the Arre deposit in the PAZ show remarkably heterogeneous sphalerite textures and related major and trace chemistry. The formation of Ge-rich minerals is mainly observed in close association with recrystallized sphalerite, so that deformation (supposed Variscan D_2) and recristallization mechanisms are likely to play a major role in the Ge concentration process (Fig. 3a); leaving behind a Ge-depleted fine grained recrystallized sphalerite matrix.

Several textural and chemical analogues to these sphalerites may be present in Chinese deformed-MVT deposits (Ye et al. 2011), in Kipushi deposits (Belissont et al. 2016; Horn et al. 2018) but also in other sulphide minerals like chalcopyrite from VHMS deposit (Reiser et al. 2011; Belissont et al. 2019). Ores affected by recrystallization are likely to contain accessory minerals that can be potentially enriched in rare metals.

Acknowledgements

The authors thank the French Geological Survey (Bureau de Recherches Géologiques et Minières; BRGM) for funding through the national program "Référentiel Géologique de France" (RGF-Pyrénées). The authors gratefully acknowledge Christophe Nevado and Doriane Delmas for the excellent thin sections preparation, Bernard Boyer and Olivier Bruguier for their involvement in EPMA and LA-ICP-MS analyses, respectively.

References

Belissont R, Munoz M, Boiron M, Luais B, Mathon O (2019) Germanium Crystal Chemistry in Cu-Bearing Sulfides from Micro-XRF Mapping and Micro-XANES Spectroscopy. Minerals 9:1–12

Belissont R, Munoz M, Boiron MC, Luais B, Mathon O (2016) Distribution and oxidation state of Ge, Cu and Fe in sphalerite by µ-XRF and K-edge µ-XANES: Insights into Ge incorporation, partitioning and isotopic fractionation. Geochim Cosmochim Acta 177:298–314.

Cook NJ, Ciobanu CL, Meria D, Silcock D, Wade B (2013) Arsenopyrite-Pyrite Association in an Orogenic Gold Ore : Tracing Mineralization History from Textures and Trace Elements. Econ Geol 108:1273–1283

Cook NJ, Ciobanu CL, Pring A, Skinner W, Shimizu M, Danyushevsky L, Saini-Eidukat B, Melcher F (2009) Trace and minor elements in sphalerite: A LA-ICPMS study. Geochim Cosmochim Acta 73:4761–4791.

Cugerone A, Cenki-Tok B, Chauvet A, Le Goff E, Bailly L, Alard O, Allard M (2018a) Relationships between the occurrence of accessory Ge-minerals and sphalerite in Variscan Pb-Zn deposits of the Bossost anticlinorium, French Pyrenean Axial Zone: Chemistry, microstructures and ore-deposit setting. Ore Geol Rev 95:1–19.

Cugerone A, Oliot E, Chauvet A, Gavalda J, Le Goff E (2018b) Structural Control on the Formation of Pb-Zn Deposits: An Example from the Pyrenean Axial Zone. Minerals 8:1–20.

Dubosq R, Lawley CJM, Rogowitz A, Schneider DA, Jackson S (2018) Pyrite deformation and connections to gold mobility : Insight from micro-structural analysis and trace element mapping. Lithos 310–311:86–104.

George LL, Cook NJ, Ciobanu CL (2016) Partitioning of trace elements in co-crystallized sphalerite-galena-chalcopyrite hydrothermal ores. Ore Geol Rev 77:97–116.

Höll R, Kling M, Schroll E (2007) Metallogenesis of germanium-A review. Ore Geol Rev 30:145–180.

Horn S, Dziggel A, Kolb J, Sindern S (2018) Textural characteristics and trace element distribution in carbonate-hosted Zn-Pb-Ag ores at the Paleoproterozoic Black Angel deposit, central West Greenland. Miner Depos 1–18.

Johan Z, Oudin E, Picot P (1983) Analogues germanifères et gallifères des silicates et oxydes dans les gisements de zinc des Pyrénées centrales, France; argutite et carboirite, deux nouvelles espèces minérales. TMPM Tschermaks Mineral und Petrogr Mitteilungen 31:97–119.

Lockington JA, Cook NJ, Ciobanu CL (2014) Trace and minor elements in sphalerite from metamorphosed sulphide deposits. Mineral Petrol 108:873–890.

Reiser FKM, Rosa DRN, Pinto ÃMM, Carvalho JRS, Matos JX, Guimaraes FMG, Alves LC, de Oliveira DPS (2011) Mineralogy and geochemistry of tin- and germanium-bearing copper ore, Barrigao re-mobilized vein deposit, Iberian Pyrite Belt, Portugal. Int Geol Rev 53:1212–1238.

Wilkinson JJ (2013) Sediment-Hosted Zinc-Lead Mineralization: Processes and Perspectives: Processes and Perspectives, Treatise on Geochemistry, Second Edition. Elsevier, H Holland, K Turekian (ed), Amsterdam, Netherlands 219–249.

Ye L, Cook NJ, Ciobanu CL, Yuping L, Qian Z, Tiegeng L, Wei G, Yulong Y, Danyushevskiy L (2011) Trace and minor elements in sphalerite from base metal deposits in South China: A LA-ICPMS study. Ore Geol Rev 39:188–217.